ADVANCES IN ATMOSPHERIC SCIENCES, VOL. 34, AUGUST 2017, 983–992

• **Original Paper** •

Aircraft Measurements of Cloud–Aerosol Interaction over East Inner Mongolia

Yuhuan LÜ*[1,2], Hengchi LEI[2,3], and Jiefan YANG[2]

[1] *Wuqing Meteorological Observatory of Tianjin, Tianjin* 301700*, China*

[2] *Key Laboratory of Cloud-Precipitation Physics and Severe Storm, Institute of Atmospheric Physics, Chinese Academy of Sciences, Beijing* 100029*, China*

[3] *Collaborative Innovation Center on Forecast and Evaluation of Meteorological Disasters, Nanjing University of Information Science and Technology, Nanjing* 210044*, China*

(Received 18 September 2016; revised 23 March 2017; accepted 1 April 2017)

ABSTRACT

To investigate the potential effects of aerosols on the microphysical properties of warm clouds, airborne observational data collected from 2009 to 2011 in Tongliao, Inner Mongolia, China, were statistically analyzed in this study. The results demonstrated that the vertical distribution of the aerosol number concentration (N_a) was similar to that of the clean rural continent. The average aerosol effective diameter (D_e) was maintained at approximately 0.4 μm at all levels. The data obtained during cloud penetrations showed that there was a progressive increase in the cloud droplet concentration (N_c) and liquid water content (LWC) from outside to inside the clouds, while the N_a was negatively related to the N_c and LWC at the same height. The fluctuation of the N_a, N_c and LWC during cloud penetration was more obvious under polluted conditions (Type 1) than under clean conditions (Type 2). Moreover, the wet scavenging of cloud droplets had a significant impact on the accumulation mode of aerosols, especially on particles with diameters less than 0.4 μm. The minimum wet scavenging coefficient within the cloud was close to 0.02 under Type 1 conditions, while it increased to 0.1 under Type 2 conditions, which proved that the cloud wet scavenging effect under Type 1 conditions was stronger than that under Type 2 conditions. Additionally, cloud droplet spectra under Type 1 conditions were narrower, and their horizontal distributions were more homogeneous than those under Type 2 conditions.

Key words: aircraft observation, aerosol, warm cloud, microphysical properties

Citation: Lü, Y. H., H. C. Lei, and J. F. Yang, 2017: Aircraft measurements of cloud–aerosol interaction over East Inner Mongolia. *Adv. Atmos. Sci.*, **34**(8), 983–992, doi: 10.1007/s00376-017-6242-z.

1. Introduction

Aerosols are an important constituent of the atmosphere, which can not only directly influence the radiation balance of the earth–atmosphere system by absorbing and scattering solar radiation (direct effect), but can also act as cloud condensation nuclei to impact the cloud optical depth, cloud lifetime, and the temporal and spatial distribution of precipitation (indirect effect; Twomey and Wojciechowski, 1969; Albrecht, 1989; Hudson and Yum, 2001, 2002; Konwar et al., 2012). However, the spatial and temporal distribution of aerosols vary widely due to the differences between ecosystems, atmospheric circulation, anthropogenic emissions and cloud processes, which in turn lead to great variations in cloud microphysical parameters. These effects induced by aerosols are too difficult to be quantified from all climatic forcing factors (IPCC, 2007). Thus, during the last decade, several in situ observations were conducted to obtain the warm cloud microphysical properties in different locations. For instance, Miles et al. (2000) compared the data measured within marine and continental strati. The results indicated the droplet number concentrations in marine clouds were lower than for continental stratus, while the mean and effective diameters for marine stratus were larger than for continental stratus. Prabha et al. (2011) compared the microphysical parameters of cumulus congestus in pre-monsoon and monsoon seasons, and found that the effective radiusat 2000 m above the cloud base between the two cases differed by up to a factor of 2 and, despite significant variations of the cloud water content in the horizontal direction, variations of the effective radius at these levels were comparatively small.

With the rapid growth in China's economy, especially the increase in heavy industries and usage of fossil fuels in North China, Beijing and surrounding areas have become an important emissions source of aerosols and cloud condensation nuclei (CCN) in East Asia. Under these circumstances, several in situ observation and modeling studies have been conducted to investigate either the direct or indirect effects of pollutants on climate change. For example, based on model

* Corresponding author: Yuhuan LÜ
Email: lvyh@tjwq.gov.cn

simulations and aircraft observations, Zhang et al. (2006) found three major sources that influence the aerosol number concentrations in North China. Aircraft observations in North China (Liu et al., 2009) indicated that high concentrations of aerosol are mainly influenced by human activities and dust storms. The microphysical properties of clouds during 2005–06 in Beijing were statistically analyzed by Deng et al. (2009) using in situ data obtained by aircraft, and the results indicated that cloud droplet number concentrations and liquid water content (LWC) in different types of clouds show substantial variations. In situ measurements over Beijing in 2008 were analyzed by Zhang et al. (2011), indicating that high LWC and high aerosol loadings can significantly alter the cloud microphysical properties in terms of cloud droplet number concentration and effective radius. However, most of the in situ observations mentioned above were conducted in heavily polluted areas. In fact, the effects of anthropogenic aerosol emissions from megacities not only impact the local environment and cloud microphysics, but also the downwind aerosol chemical composition and cloud microphysical properties through long-range transportation under specific atmospheric circulations (Jaffe et al., 2003; Adhikari et al., 2005).

The way in which pollutants over mainland East Asia affect the optical and microphysical properties of clouds over local and surrounding areas is a long-standing problem and, until now, the availability of data has been insufficient to provide explicit answers. Therefore, the potential climate impacts also need further study. More detailed observations of aerosol–cloud interaction in different regions are crucial. In this context, the present study examined the vertical distributions of aerosols, the microphysical properties of clouds, and the wet scavenging process, to investigate aerosol–cloud interaction over East Inner Mongolia—a region downwind of cities like Beijing, and therefore possibly affected by their heavy levels of pollution.

2. Methods and data

2.1. *Flight information*

From 2009 to 2011, several observational flights were conducted by the Laboratory of Cloud-Precipitation Physics and Severe Storms, Institute of Atmospheric Physics, associated with Tongliao Meteorological Bureau. The main purpose of those in situ observations was to investigate aerosol–cloud interactions in the downwind area of heavily polluted megacities, such as Beijing. Most of the observations were made in Tongliao City and its surrounding area within a 50-km range (Fig. 1), which is in the eastern part of Inner Mongolia Province and the western part of the Songliao Plain. It is an arid and semi-arid region and approximately 600 km northeast of Beijing. The southern and northern edges of the study area are surrounded by high terrain, while its center is a low-lying area mainly covered by sands and dunes. Tongliao has a typical temperate continental climate, with an interchange of westerlies and subtropical airflow, whose precipitation is mainly influenced by the surrounding terrain

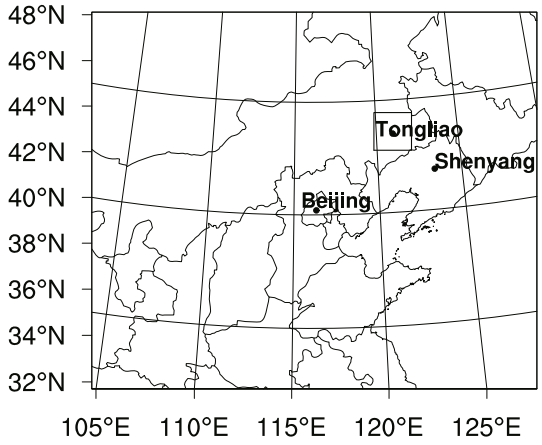

Fig. 1. Location of Tongliao. The black rectangle denotes the study area.

as well as mesoscale synoptic systems, such as westerly troughs, cold fronts, warm fronts and midlatitude cyclones. Moreover, under the effect of low-level southwesterly flow in front of low pressure systems, the study area is usually affected by long-range pollutant transport from North China, which results in rapid increases in aerosol number concentrations. In this study, 41 aircraft measurements of aerosols and data obtained during cloud penetrations were utilized to study aerosol–cloud interactions.

2.2. *Instrumentation on the aircraft*

Airborne instruments employed in the observations were mounted on a multi-engine aircraft (Y-12) by the Tongliao Weather Modification Office to measure the number concentration and size spectra of particles and meteorological parameters, as well as the spatial locations simultaneously. The size spectra of particles were obtained by a particle measuring system (DMT Inc., Boulder, CO, USA), including a Passive Cavity Aerosol Spectrometer Probe (PCASP) and a Cloud and Aerosol Spectrometer (CAS). Small and medium-sized particles, with diameters ranging from 0.1 to 3.0 μm, such as sulfate, organic carbon, soot and smaller mineral dust particles, were recorded by the PCASP with 30 unequally sized bins. The CAS instrument, with 30 unequally sized bins, was applied to measure large aerosol particles under clear-sky conditions or small cloud droplets, with diameters ranging from 0.6 to 50 μm within clouds. To avoid the influence of large aerosols, only particles with diameters larger than 3 μm were counted as cloud droplets. The LWC measured during cloud penetration was derived based on the volume concentration of cloud droplets, with an assumption that all the droplets were spherical. The meteorological parameters, including temperature, relative humidity, pressure and wind direction, were obtained using an AIMMS-20 (Aircraft Integrated Meteorological Measurement System, Advantech Research Inc., Barrie, Canada). All the measurements were performed at a 1-Hz sample rate on a Y-12 aircraft with a true air speed of approximately 50 m s^{-1}, and most of the flight observations were performed below an altitude of 6 km.

2.3. *Theory and method*

The number concentrations of particles with different diameters were recorded by the PCASP and CAS probes, and each instrument had 30 size bins.

The total number concentration ($N_{\rm tot}$) for each instrument is the sum of the concentration from all bins, which is expressed by

$$N_{\rm tot} = \sum_{i=1}^{n} N_i \ . \tag{1}$$

By assuming all of the cloud droplets are spherical, the parameters such as LWC and effective diameter ($D_{\rm e}$) can be expressed as follows:

$$\mathrm{LWC} = \sum_{i=1}^{n} n_i D_i^3 \rho_w \frac{\pi}{6} \ , \tag{2}$$

$$D_{\rm e} = \frac{\sum\limits_{i=1}^{n} n_i D_i^3}{\sum\limits_{i=1}^{n} n_i D_i^2} \ , \tag{3}$$

where n_i represents the particle numbers observed in the ith bin of the PCASP or CAS, D_i means the geometrical mean diameter at the ith bin, N_i (cm^{-3}) is the particle number concentration at the ith bin, and $\rho_{\rm w}$ = 1 g cm^{-3} stands for the density of liquid water.

2.4. *Data selection and processing*

According to previous studies, there were several criteria utilized to define the cloud area on the basis of the data obtained by different instruments. For instance, some researchers have used the number concentration (> 10 cm^{-3}) of cloud droplets derived from the Forward Scattering Spectrometer Probe (FSSP) as a threshold (Rangno and Hobbs, 2005; Stith et al., 2006); Gultepe et al. (1996) proposed the LWC measured by the Hotwire-LWC probe (LWC > 0.01 g m^{-3}) or a combination of the FSSP number concentration and the LWC ($N_{\rm c}$ > 0.1 cm^{-3} and LWC > 0.0005 g m^{-3}) (Gultepe and Isaac, 2004) as a criterion; Zhang et al. (2011) used $N_{\rm c}$ > 10 cm^{-3} and LWC > 0.001 g m^{-3}. Liu et al. (2009) proposed a criterion of $N_{\rm c}$ > 10 cm^{-3} and RH > 70% to distinguish cloudy areas from cloudless ones. Notably, there are still large uncertainties in defining the cloud area due to the accuracy of instruments used in this study. Thus, based on the methods mentioned above, and to minimize the uncertain factors, such as instrument error, the occurrence of clouds was determined in the present study according to the following thresholds: $N_{\rm c}$ > 10 cm^{-3} and LWC > 0.001 g m^{-3}.

To minimize the ambiguity and investigate the potential effects of different criteria on aerosol distributions, we carried out a sensitivity test by slightly altering the criteria for selecting aerosols. The aerosol data were selected based on three thresholds: (1) $N_{\rm c}$ < 10 cm^{-3}; (2) $N_{\rm c}$ < 0.1 cm^{-3} and LWC < 0.0005 g m^{-3}; (3) $N_{\rm c}$ < 10 cm^{-3} and LWC < 0.001 g m^{-3}. We selected two cases to compare the characteristics of aerosols under the corresponding criteria. The results indicated that the characteristics of aerosols have no obvious difference, which is consistent with previous studies (e.g., Konwar et al., 2015). Therefore, we concluded that the effects of different criteria on the vertical distributions and aerosol spectra were very small.

Because the aircraft could not penetrate cumuli congestus, only cumulus humilis were involved in this work—a cumulus cloud type with a smaller vertical and horizontal extent compared to convective cloud. The horizontal scales of these clouds were mostly several hundred meters, with only a few of them extending to one or two kilometers. They had limited depth (technically known as showing no significant vertical development), and were typically found at lower levels (500–3000 m). Moreover, flight observations were mainly conducted in the warm region of the clouds, with flight altitudes of 1–4 km. The cloud type was determined by the flight log.

To avoid the influence of the wet scavenging effect of raindrops, data measured during precipitation were excluded, based upon the flight diary. The selected vertical profile data measured during the ascent or descent of the aircraft were used to reveal the characteristics of the vertical distribution of aerosols.

3. Basic statistical characteristics of aerosols

3.1. *Vertical distributions of aerosol number concentration*

Figure 2 shows that the aerosol number concentration ($N_{\rm a}$) generally decreased exponentially with increasing altitude, which can be expressed by the following classical exponential form:

$$N_{\rm a} = N_0 \exp\left(-\frac{H}{H_{\rm p}}\right) , \tag{4}$$

where H, N_0 (1785 cm^{-3}) and $H_{\rm p}$ (1733 m) represent altitude, the aerosol number concentration near the surface and the scale height, respectively. Regression analysis revealed that the determination coefficient (R^2) and the root mean square error (RMSE) were 0.9614 and 83.67, respectively. Figure 2 also shows that the aerosol number concentration near the surface over the Tongliao region varied significantly, with an average value of approximately 1800 cm^{-3}. Collins et al. (2000) found that total number concentrations increased to greater than 1000 cm^{-3} and, for the most polluted case, exceeded 4000 cm^{-3}. The fitting curve of the vertical profile of the average aerosol number concentration, $N_{\rm a-Fit}$, was consistent with the clean continental aerosol vertical profile suggested by a previous study (Seinfeld and Pandis, 1997). However, it was greatly different from that observed in Beijing and its surrounding areas [N_0 = 6600 cm^{-3}, $H_{\rm p}$ = 1419 m, R^2 = 0.9881, RMSE = 247 cm^{-3} (Liu et al., 2009)], which are substantially influenced by anthropogenic emissions. The aerosol number concentrations in Tongliao are usually less than those over the Beijing area, at all levels, particularly within the boundary layer.

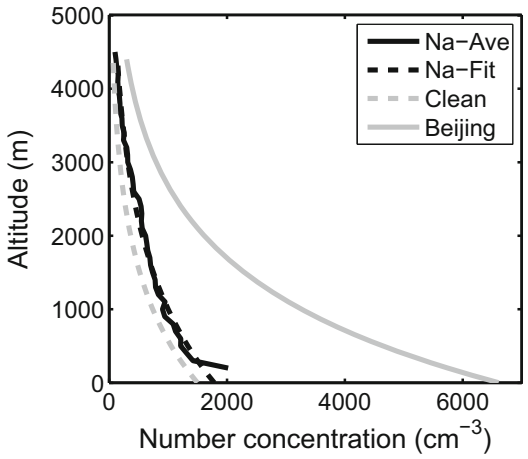

Fig. 2. Vertical profiles of N_a. The solid black line, dashed black line, dashed gray line, and solid gray line represent the average N_a vertical profile, the line fitted to the average N_a vertical profile, the line fitted to the average N_a vertical profile under clean conditions (suggested by Seinfeld and Pandis, 1997), and the line fitted to the average N_a vertical profile in Beijing (the result of Liu et al., 2009), respectively.

3.2. *Characteristics of the aerosol size distribution*

The vertical distributions of the aerosol effective diameter, D_e (presented in Fig. 3a), clearly indicate that the values of D_e ranged from 0.3 to 0.6 μm at each altitude level. We analyzed the 10th and 90th percentiles of data at each altitude level (expressed in error bars). Meanwhile, the average D_e decreased with increasing height within the boundary layer and further decreased in the free atmosphere. The average D_e values at all levels were slightly smaller than those over Beijing (Liu et al., 2009), where the average D_e increases slightly with altitude. This difference may be attributable to the sudden occurrence of a sand storm during observations in areas around Beijing. In our study, the aerosols were mainly produced by the gas–particle conversion process, and affected by the long-range transport of pollutants from North China; whereas, the influence of dust was less important, resulting in the smaller size of aerosols and a decrease in D_e with height.

The average aerosol particle size distributions from the CAS and PCASP, at the different altitudes of 200 m, 1000 m, 2000 m and 3000 m (Fig. 3b), illustrate that the shapes of the size distributions of particles at different levels were very similar. For the PCASP, all of them were composed of two particle modes, with the smaller mode peaking at 0.3 μm and the larger mode peaking at a maximum value of 0.7 μm. The relative contributions of particles between 0.3 and 2 μm to the total aerosol number concentration near the surface level (200 m) were larger than those at upper levels (1000 m, 2000 m, 3000 m). Besides, the shapes of the size distributions at high altitude (2000 m and 3000 m) were almost the same. The similarity of the size spectra at different levels also indicates that the aerosols at different altitudes—primarily small particles with diameters less than 0.3 μm—may generally have been from the same source. A comparison of the observational

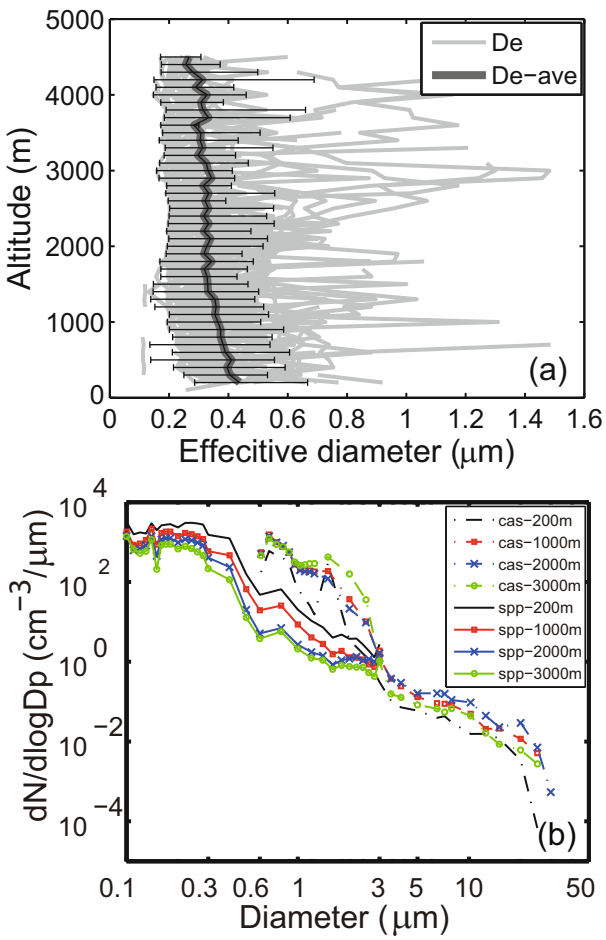

Fig. 3. (a) All vertical profiles of D_e. The solid gray lines represent the observed D_e, and the solid black line represents the vertical profile of the average D_e. The 10th and 90th percentiles of data at each altitude level are expressed as error bars. (b) Comparison of average aerosol particle size distributions from the CAS and PCASP, at altitudes of 200 m, 1000 m, 2000 m and 3000 m.

data collected in Beijing (Liu et al., 2009) and our study suggests that the relative contributions of large particles to the total aerosol number concentrations was relatively small in this case, which means the long-range transport of large particles, such as dust, in the free troposphere, was less important during the observations.

In addition, the aerosol size spectra obtained simultaneously by the CAS and PCASP also indicated that there were obvious differences between the CAS- and PCASP-observed aerosol spectra in the overlap region (0.6–3 μm). Generally, for measurements near the ground layer, the difference between the two instruments was relatively small, but the discrepancy increased with increasing height. Collins et al. (2000) showed that significant discrepancies can occur in the overlapped particle size range of the FSSP and the PCASP. These discrepancies can be attributed to the lack of unique particle sizes corresponding to certain values of scattered intensity, as well as the nonspherical aerosol particles. Thus, based on the intercomparison between the data

obtained from the PCASP and CAS alone, it is very difficult to confirm whether the peaks found in the PCASP data were artifacts, since the two instruments have the same problem in determining aerosol size. It is smaller when compared with the PCASP and FSSP observational results of Collins et al. (2000), but the trend is basically consistent. Collins et al. (2000) simply proposed that the consistent agreement between the FSSP and PCASP at approximately 2.5 μm can be used as a cutoff size, below which the PCASP data can be assumed as more accurate, and above which the FSSP data are more accurate. We also realized that the peaks in the PCASP data may be unreliable but, until now, quantitative studies of this instrument are still very scarce.

4. Characteristics of warm cloud

4.1. *Classification of data*

To investigate aerosols and the microphysical properties of clouds under different conditions, observational data obtained during the field campaign were divided into two categories based on weather patterns. Under the first condition (hereafter referred to as Type 1), the observation area was in front of an upper trough with a low-pressure system. The lower atmosphere of the observation area was dominated by a southwesterly wind and the air mass contained relatively abundant water vapor and pollutants from North China. The pollutants from that region, carried by the southwesterly wind, had a considerable impact on the aerosol number concentration in the observation region (Table 1). Under the second condition (hereafter referred to as Type 2), the observation area was in front of an upper trough or behind a northeasterly cyclone. Therefore, the air mass was relatively dry, while the low-level wind direction was mainly northwesterly and northerly. Under this situation, aerosols mainly came from remote continental areas, such as Northwest China, Mongolia and Siberia, resulting in lower aerosol number concentrations in the observation region compared with Type 1 (Table 2). Discrepancies between the two weather patterns, including low-level aerosol number concentrations, moisture and updrafts, led to different microphysical properties of clouds. Moreover, to represent the horizontal variation of clouds and aerosols during the cloud penetrations, the data obtained from outside to inside of the clouds were categorized into three parts: outside the cloud; lateral boundary of the cloud; and within the cloud. All are marked in Fig. 4

Table 1. Statistical characteristics of clouds and aerosols under polluted conditions (Type 1).

Case	Height (m)	T (s)	$N_{a,1}$	$N_{a,2}$	$N_{a,3}$	$N_{c,2}$	$N_{c,3}$	LWC_2	LWC_3
1-1	3190	36	1095	564	260	428 ± 168	1196 ± 296	0.0091	0.0283
1-2	3190	26	1102	375	312	767 ± 300	997 ± 262	0.0185	0.0239
1-3	3220	84	1107	643	203	260 ± 194	1078 ± 271	0.0057	0.0264
1-4	3180	35	1284	891	294	156 ± 219	916 ± 237	0.0036	0.0255
1-5	3130	64	1152	763	322	191 ± 121	698 ± 149	0.0044	0.0182
Average			1200	645	279	360 ± 200	977 ± 243	0.008	0.025

Notes: T, time during cloud penetration; $N_{a,1}$, mean aerosol number concentration (cm^{-3}) outside the cloud; $N_{a,2}$, mean aerosol number concentration (cm^{-3}) in the lateral boundary of the cloud; $N_{a,3}$, mean aerosol number concentration (cm^{-3}) within the cloud; $N_{c,2}$, cloud droplet concentration (cm^{-3}) and standard deviation in the lateral boundary of the cloud; $N_{c,3}$, cloud droplet concentration (cm^{-3}) and standard deviation within the cloud; LWC_2, liquid water content ($g\ m^{-3}$) in the lateral boundary of the cloud; LWC_3, liquid water content ($g\ m^{-3}$) within the cloud.

Table 2. Statistical characteristics of clouds and aerosols under polluted conditions (Type 2).

Case	Height (m)	T (s)	$N_{a,1}$	$N_{a,2}$	$N_{a,3}$	$N_{c,2}$	$N_{c,3}$	LWC_2	LWC_3
2-1	2900	16	215	193	75	46 ± 47	78 ± 8	0.00095	0.0015
2-2	2920	24	67	43	24	79 ± 68	233 ± 60	0.0016	0.0049
2-3	2900	38	36	30	11	30 ± 22	304 ± 69	0.00084	0.0077
2-4	3150	84	64	41	24	54 ± 44	338 ± 108	0.0029	0.0138
2-5	3940	21	103	85	29	28 ± 30	96 ± 41	0.0019	0.0079
2-6	3460	15	301	284	257	17 ± 15	114 ± 70	0.00072	0.0074
2-7	3390	43	279	247	146	24 ± 24	100 ± 26	0.002	0.0086
2-8	3380	155	301	190	161	77 ± 40	184 ± 32	0.007	0.029
2-9	3920	37	84	48	30	23 ± 19	59 ± 16	0.0017	0.0025
2-10	3550	22	180	127	72	25 ± 32	193 ± 67	0.0054	0.0122
2-11	3510	30	237	105	47	73 ± 65	207 ± 52	0.0032	0.0058
Average			177	122	80	45 ± 39	177 ± 21	0.0026	0.0091

Notes: T, time during cloud penetration; $N_{a,1}$, mean aerosol number concentration (cm^{-3}) outside the cloud; $N_{a,2}$, mean aerosol number concentration (cm^{-3}) in the lateral boundary of the cloud; $N_{a,3}$, mean aerosol number concentration (cm^{-3}) within the cloud; $N_{c,2}$, cloud droplet concentration (cm^{-3}) and standard deviation in the lateral boundary of the cloud; $N_{c,3}$, cloud droplet concentration (cm^{-3}) and standard deviation within the cloud; LWC_2, liquid water content ($g\ m^{-3}$) in the lateral boundary of the cloud; LWC_3, liquid water content ($g\ m^{-3}$) within the cloud.

(an example of cloud penetration). The outside-cloud data are the light-gray regions, in which the cloud droplet number concentrations measured by CAS were 0. The lateral boundary is the region of the cloudy area mixed with cloudless gaps due to the entrainment of dry air and the combination of thermal bubbles. Thus, it could be subjectively identified based on the values and fluctuations of N_c. For example, the lateral boundary of the cloud could be identified as where the N_c was lower than in the cloud core areas, and fluctuated more, due to the mixing and dilution processes induced by the entrainment of dry air (medium-gray area in Fig. 4). The within-cloud region (marked by the dark-gray area in Fig. 4) was defined as the region between two cloud lateral boundaries, where the dry air entrainment may have been less important and convective regions developed more vigorously than in the other parts.

4.2. *Statistical characteristics of cloud and aerosols*

The results shown in Tables 1 and 2 show that, prior to and after the cloud penetrations, the aerosol concentration decreased noticeably, while both the cloud droplet concentration and the LWC increased. The average aerosol number concentration in the lateral boundary under the Type 1 and Type 2 conditions was 645 cm^{-3} and 122 cm^{-3}, respectively, which is consistent with other previous observations (e.g., Collins et al., 2000; Konwar et al., 2015). The average cloud droplet number concentration of the cloud core under the Type 1 and Type 2 conditions was 977 ± 243 cm^{-3} and 177 ± 21 cm^{-3}, respectively, while the LWC was 0.025 g cm^{-3} and 0.0091 g cm^{-3}, respectively. Compared with the observational results of the FSSP at Beijing in the same period (Deng et al., 2009), the average N_c in our results was larger and the average LWC was smaller. However, the average LWC for different places, summarized by Miles et al. (2000), ranged from 0.005 to 0.9 g cm^{-3}. They compared the data measured within marine and continental strati and found that the average cloud droplet number concentration

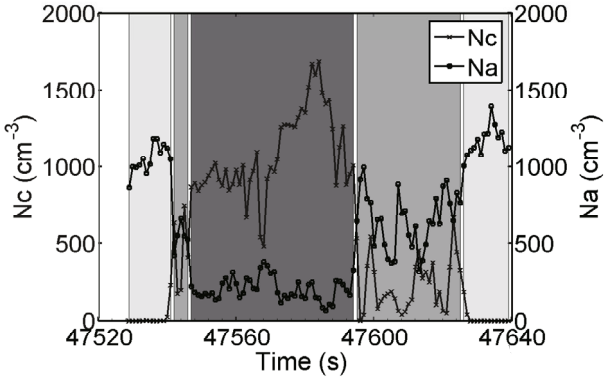

Fig. 4. An example of the variation in N_a and N_c during cloud penetration. The within-cloud region is shaded dark-gray, and there are two zones outside of the within-cloud region identified: the lateral boundary is the region represented by the medium-gray shading, and the outside-cloud regions are shaded light-gray, where the N_c measured by CAS was 0.

was 74 ± 45 cm^{-3} and 288 ± 159 cm^{-3}, respectively. Comparison of the statistics measured under Type 1 and Type 2 conditions reveals that the aerosol number concentration (N_a) was negatively correlated with N_c and LWC from the outside-cloud to within-cloud locations at the same height. Meanwhile, the within-cloud standard deviation of N_c was larger than that at the lateral boundary of the cloud, and the LWC at the lateral boundary was much smaller than within the cloud. This result could be simply attributed to the evaporation of cloud droplets within the under-saturated condition produced by dry-air entrainment. However, there are still some discrepancies between the two conditions. For instance, the average N_a outside of the cloud in Type 1 weather was mostly much larger than that under Type 2 weather, because of the long-range transport of aerosols. Figure 5 shows that the values of N_a decreased from 1200 cm^{-3} to 279 cm^{-3} from the outside- to within-cloud regions. The ratio of the N_a within the cloud to that outside the clouds was 0.23 under Type 1 conditions, while under Type 2 conditions it was 0.68. This result shows that the ratio of N_a within clouds to that outside of clouds may partially depend on the aerosol loading, as suggested by several previous field observations (e.g., Hallberg et al., 1994). Another significant difference between the two types was that the cloud droplet number concentration, N_c, was larger under the Type 1 conditions than under the Type 2 conditions, indicating that more aerosols were activated under the Type 1 conditions.

4.3. *Cloud droplet spectra*

Generally, clouds that form in air masses with higher CCN concentrations, affected by anthropogenic sources, tend to have smaller droplets compared to those formed under clean conditions (Twomey and Wojciechowski, 1969; Albrecht, 1989; Hobbs and Rangno, 1998; Hudson and Yum, 2001). In the present study, as shown in Fig. 6, the cloud droplet size distribution in each case under polluted conditions (Type 1) was more uniform, and the diameters of cloud droplets were usually less than 8 μm. Furthermore, the number concentration of smaller droplets (diameter < 3 μm) was greater than 1000 cm^{-3}, while that of larger droplets (diameter > 8 μm) was less than 1 cm^{-3}. In contrast, under clean conditions (Type 2), although the number concentration of smaller droplets (diameter < 5 μm) was smaller than under Type 1 conditions by an order of magnitude, the concentration of larger particles (diameter > 8 μm) was larger than that under Type 1 conditions, again by an order of magnitude, due to the wider spectra of cloud droplets. This agrees with the finding of Hudson and Yum (2001), who compared averages of cloud droplet spectra in maritime and continental clouds at different altitudes. They found there were more large (diameter > 30 μm) cloud droplets (by an order of magnitude) for maritime flights.

The results discussed above reveal that the cumulus clouds that formed under polluted conditions contained a larger cloud number concentration, with a smaller cloud droplet size and narrower size spectra. In contrast, under clean conditions, the cloud droplet number concentration was

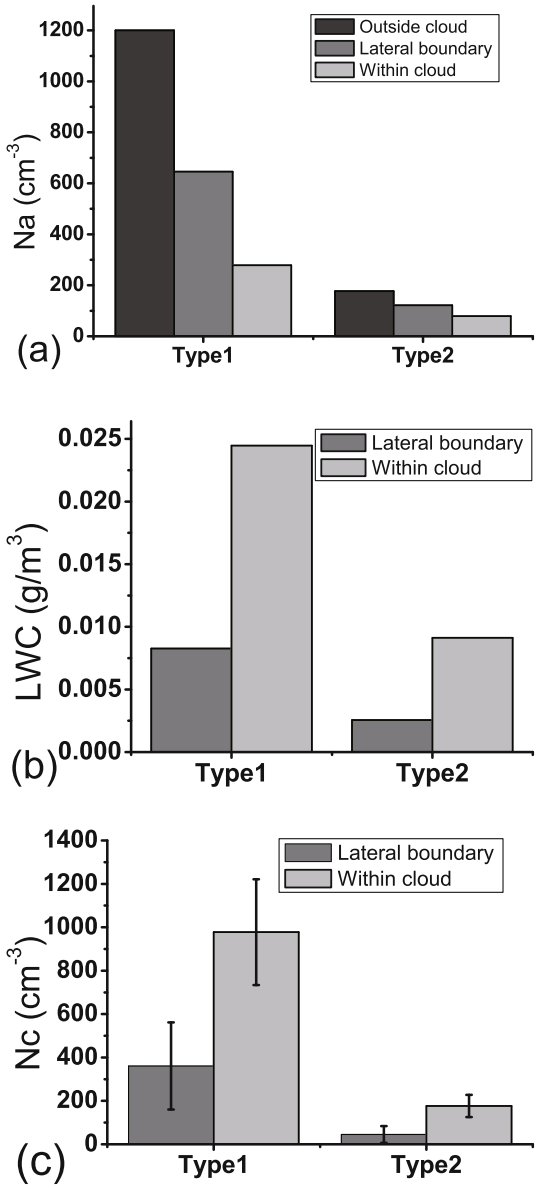

Fig. 5. Comparison of average values of N_a, LWC and N_c under Type 1 and Type 2 conditions in different regions: (a) N_a for the regions outside the cloud, at the lateral boundary of the cloud, and within the cloud; (b) LWC for the regions at the lateral boundary of the cloud, and within the cloud; (c) N_c and standard deviation (expressed as vertical error bars) for the regions at the lateral boundary of the cloud, and within the cloud.

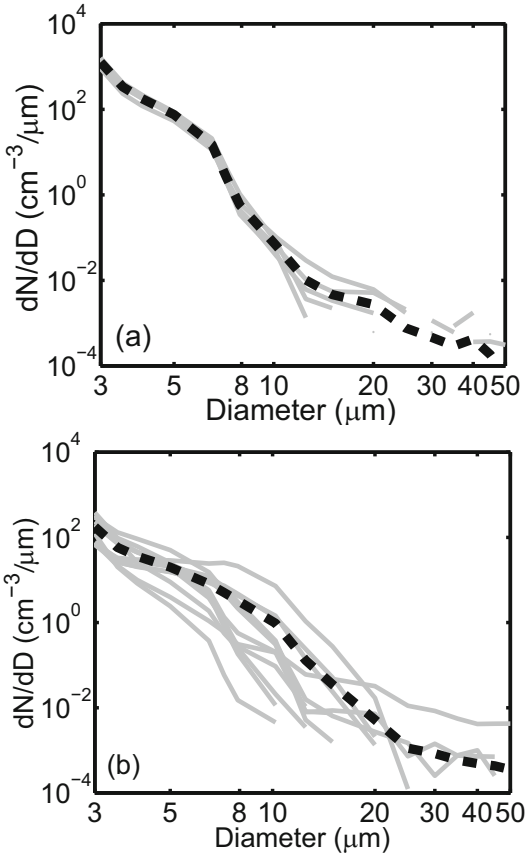

Fig. 6. Cloud droplet size distribution under two different types. The solid gray lines represent the observed cloud droplet size distribution for each case, and the black dotted lines represent the average cloud droplet size distribution under (a) Type 1 (polluted conditions) and (b) Type 2 (clean conditions).

smaller, but with more large droplets and a wider size spectrum than that under polluted conditions. This result is not only consistent with that demonstrated in previous studies (e.g., Twomey and Wojciechowski, 1969; Albrecht, 1989; Hobbs and Rangno, 1998), but also to recent observations of aerosol–cloud interaction conducted during the same period in India (Konwar et al., 2012) and in North China (Zhang et al., 2011). Konwar et al. (2012) analyzed the microphysical properties of clouds at various altitudes during the Cloud Aerosol Interaction and Precipitation Enhancement Experiment, and reported that greater CCN concentrations give rise to clouds with smaller drops and greater cloud droplet number concentrations. By comparing the in situ aircraft measurements of clouds and aerosols of seven flights over the Beijing region, Zhang et al. (2011) demonstrated that the cloud droplets, which were sensitive to LWC, increased from 700 to 1900 cm^{-3} when aerosol particles increased from 1000 to 6000 cm^{-3}.

4.4. *Horizontal distributions of cloud droplet spectra*

There was a noteworthy difference in the horizontal distribution of the cloud droplet spectra under the two weather conditions (Fig. 7). Under polluted conditions, droplet spectra were mostly narrower, and cloud droplets with diameters greater than 15 μm were very rare compared to those under clean conditions. This could be attributable to the activation of several aerosols and competition between the condensational growth of droplets. The cloud droplet spectra distributions under the Type 1 conditions were more homogeneous than under the Type 2 conditions. That is, a broadening of droplet spectra during cloud penetration from the cloud boundary to within the cloud was not obvious under Type 1 conditions. These results demonstrate that the dry-air entrainment at the cloud lateral boundary may have had less

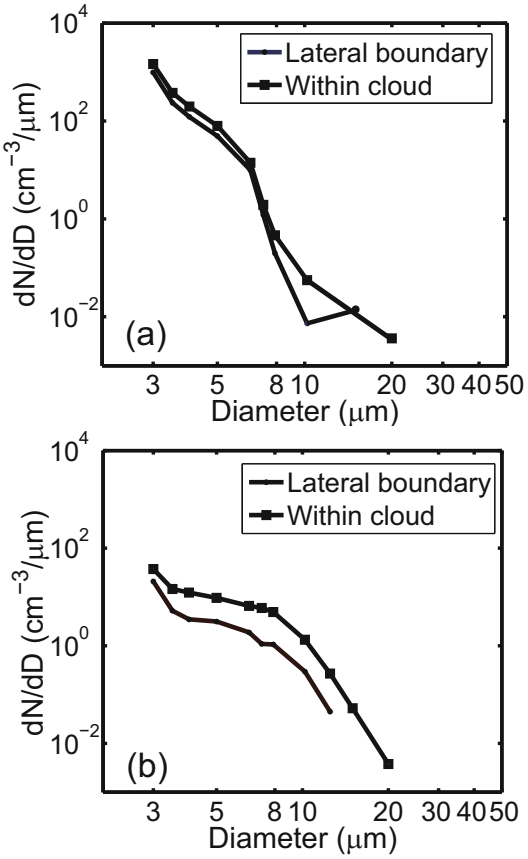

Fig. 7. Horizontal distribution of cloud droplet spectra in the lateral boundary of the cloud and within the cloud, under (a) Type 1 (polluted conditions) and (b) Type 2 (clean conditions).

impact on the droplet spectra under the Type 1 conditions than under the Type 2 conditions. The horizontal distribution of the cloud droplet spectra under the Type 2 conditions varied greatly, and more large droplets could be found within the cloud than in the cloud boundary region. Thus, it seems that dry-air entrainment had a substantial effect on the droplet spectra, due to the rapid evaporation of cloud particles, under the Type 2 conditions.

5. Cloud wet scavenging of aerosols under the two conditions

A decline in the aerosol number concentration is mainly due to the effect on aerosols of cloud wet scavenging, including the activation of larger aerosols as CCN and the collision of cloud droplets with smaller aerosols via Brownian motion. For accumulation-mode aerosols, activation is the dominant process leading to the transformation between aerosols and cloud droplets; while for small particles, other processes, such as coagulation induced by Brownian motion, are more significant in reducing the number concentration of aerosols. The latter process is probably only important in terms of changing the number concentration of Aitken nuclei, while the former process is critical in determining the cloud droplet number concentration. Although the activation process is relatively well known, wet scavenging of particles in actual clouds is complex and not well understood. To quantify the differences in the cloud wet scavenging effect on particles with different sizes under the two conditions, two specific cases were examined.

According to Noone et al. (1992), a wet scavenging coefficient, which is used to describe the wet scavenging effects on aerosols, can be expressed as follows:

$$F_{N,i} = \frac{N_{i,\text{in-cloud}}}{N_{i,\text{out-cloud}}}\,, \tag{5}$$

where $N_{i,\text{in-cloud}}$ and $N_{i,\text{out-cloud}}$ represent the particle number concentration in the ith bin, as measured by the aerosol probe (PCASP) within and outside the cloud, respectively. The smaller the value of $F_{N,i}$, the more aerosols are scavenged. Figure 8 reveals that the effect of cloud wet scavenging under the two different weather conditions was concentrated on the accumulation-mode aerosols, especially on particles with diameters less than 0.4 μm. However, the wet scavenging effect under polluted conditions was stronger than that under clean conditions. Under polluted conditions, the minimum wet scavenging coefficient within clouds was close to 0.04, suggesting that 96% of aerosol particles were eliminated by the process of cloud wet scavenging; while under clean conditions, it was close to 0.1. This result agrees with other previous observations (e.g., Gillani et al., 1995; Noone et al., 1992). For small particles (0.1–0.14 μm), the scavenging effects under both weather conditions were quite similar, with $F_{N,i}$ values of approximately 0.3, suggesting approximately 70% of the aerosols were scavenged by activating as CCN. Another part of the non-soluble particles, though difficult to be activated as CCN, were mainly adsorbed by cloud droplets, due to the diffusion–collision induced by Brownian motion. The cloud scavenging effect on the accumulation-mode aerosol particles of 0.15–0.3 μm was most obvious under both conditions, since the $F_{N,i}$ values were between 0.04 and 0.3, indicating that this group of particles were the main source of CCN. However, the $F_{N,i}$ under Type 2 increased in the same size range by a factor of 10 compared to that under Type 1, suggesting that the wet scavenging, in terms of activation, may partially have depended on the aerosol loading as well as the corresponding thermal dynamic situation. Note that, for large aerosols with diameters ranging from 0.3 to 1 μm, the $F_{N,i}$ increased rapidly with the increasing size of aerosol particles within clouds, with a maximum value exceeding 1. The $F_{N,i}$ further increased by a factor of 10–100 for particles with sizes ranging from 1 to 3 μm. This was simply because many small aerosols become larger aerosols via hygroscopic growth or activation processes, such that the number concentrations of coarse-mode particles within clouds were much larger than those outside clouds.

6. Summary and discussion

Based on a statistical analysis of in situ observation data obtained using airborne instruments during 2009–11 over the

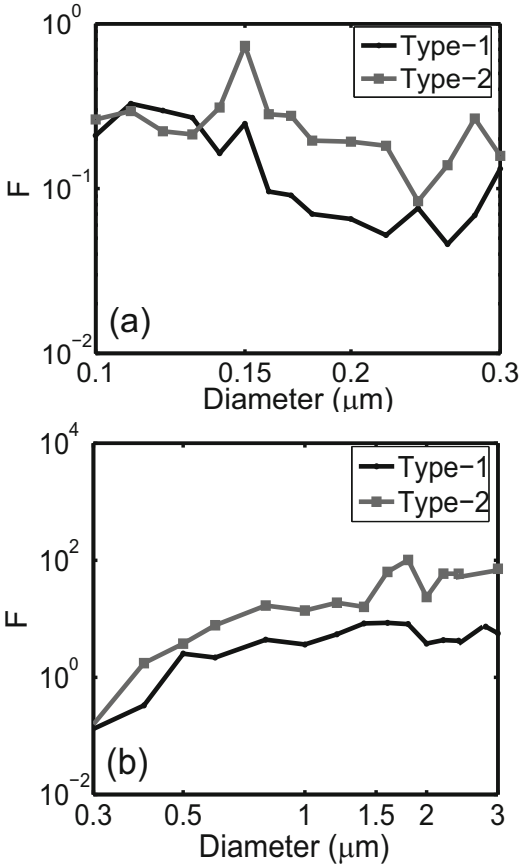

Fig. 8. The average $F_{N,i}$ for different aerosol diameters within clouds: (a) 0.1–0.3 μm; (b) 0.3–3μm. The lines with circular and square data points are for Type 1 (polluted conditions) and Type 2 (clean conditions), respectively.

Tongliao area, the following results were found: (1) The aerosol vertical distributions of the Tongliao region varied largely from case to case, but the mean profile, which was similar to that of the classical clean continent type, indicated that the aerosol number concentration was much smaller than that measured in heavily polluted regions, such as Beijing and its surrounding areas, at different levels.

(2) The average effective diameter (D_e) basically remained at approximately 0.4 μm, but decreased from near the ground to the upper air. The similarity in the size spectra at different levels indicated that the aerosols, primarily small particles with diameters less than 0.3 μm, at different altitudes, may mostly have come from the same source, while the long-range transport of large particles, such as dust, in the free troposphere, was less important during the observations.

(3) Data obtained during cloud penetrations revealed that, under both weather types, N_a decreased from outside to within the cloud, with an increase in N_c and LWC at the same height. Due to the evaporation, as well as the mixing processes induced by the entrainment of dry air, the LWC and N_a of the lateral boundary of the cloud was much smaller than that within the cloud. Generally, comparison between microphysical properties obtained under polluted and clean conditions revealed similar results to many previous studies.

(4) The cloud microphysical properties in terms of LWC, cloud droplet number concentration and size spectra, were substantially altered by the weather type. The cumulus clouds that formed under polluted weather conditions (Type 1) contained many cloud droplets of small size. In contrast, under clean conditions (Type 2), the cloud droplet number concentrations were smaller, while the cloud droplet spectra were wider compared to those under Type 1 conditions. In addition, the cloud droplet concentration and width of the size spectra were closely related to the aerosol number concentration.

(5) There was a considerable difference in terms of the horizontal distribution of the cloud droplet spectra between the two conditions. Under Type 1, the cloud droplet spectra distribution was more homogeneous, suggesting that the dry-air entrainment at the lateral boundary may have had little influence on the droplet spectra. In contrast, the horizontal distribution of cloud droplet spectra under Type 2 conditions varied greatly. More large droplets and wider spectra were captured within the cloud compared with in the cloud lateral boundary region, suggesting that cloud lateral boundary entrainment may have had a greater effect on droplet spectra under this condition.

(6) Wet scavenging was also investigated under the two weather types, and the results indicated that this process was more obvious under polluted conditions than under clean conditions. The effect of cloud wet scavenging on aerosols was mainly concentrated on the accumulation-mode particles, especially those with a diameter less than 0.4 μm. It should be noted that, limited by the flight pattern and low temporal resolution (1 Hz), data for the sub-cloud layer were not obtained, and the cloud lateral boundary could not be discerned accurately. Thus, the related conclusion regarding wet scavenging presented in this paper is a preliminary one. We intend to address these problems in future work.

Acknowledgements. This study was jointly supported by the Strategic Priority Research Program of the Chinese Academy of Sciences (Grant No. XDA05100304) and the Chinese Natural Science Foundation (Grant No. 41005073). The authors express thanks to the aircraft observations team of the China Fly Dragon Special Aviation Company, and the Weather Modification Office at Tongliao Meteorology Bureau.

REFERENCES

Adhikari, M., Y. Ishizaka, H. Minda, R. Kazaoka, J. B. Jensen, J. L. Gras, and T. Nakajima, 2005: Vertical distribution of cloud condensation nuclei concentrations and their effect on microphysical properties of clouds over the sea near the southwest islands of Japan. *J. Geophys. Res.*, **110**(D10), D10203, doi: 10.1029/2004JD004758.

Albrecht, B. A., 1989: Aerosols, cloud microphysics, and fractional cloudiness. *Science*, **245**, 1227–1230, doi: 10.1126/science.245.4923.1227.

Collins, D. R., and Coauthors, 2000: In situ aerosol-size distribu-

tions and clear-column radiative closure during ACE-2. *Tellus B*: *Chemical and Physical Meteorology*, **52**(2), 498–525, doi: http://dx.doi.org/10.3402/tellusb.v52i2.16175.

Deng, Z. Z., C. S. Zhao, Q. Zhang, M. Y. Huang, and X. C. Ma, 2009: Statistical analysis of microphysical properties and the parameterization of effective radius of warm clouds in Beijing area. *Atmos. Res.*, **93**, 888–896, doi: 10.1016/j.atmosres.2009.04.011.

Gillani, N. V., S. E. Schwartz, W. R. Leaitch, J. W. Strapp, and G. A. Isaac, 1995: Field observations in continental stratiform clouds: Partitioning of cloud particles between droplets and unactivated interstitial aerosols. *J. Geophys. Res*., **100**(D9), 18 687–18 706, doi: 10.1029/95JD01170.

Gultepe, I., G. A. Isaac, W. R. Leaitch, and C. M. Banic, 1996: Parameterizations of marine stratus microphysics based on in situ observations: Implications for GCMs. *J. Climate*, **9**(2), 345–357, doi: 10.1175/1520-0442(1996)009<0345:POMSMB>2.0.CO;2.

Gultepe, I., and G. A. Isaac, 2004: Aircraft observations of cloud droplet number concentration: Implications for climate studies. *Quart. J. Roy. Meteor. Soc*., **130**, 2377–2390, doi: 10.1256/qj.03.120.

Hallberg, A., and Coauthors, 1994: Phase partitioning of aerosol particles in clouds at Kleiner Feldberg. *Journal of Atmospheric Chemistry*, **19**, 107–127, doi: 10.1007/BF00696585.

Hobbs, P. V., and A. L. Rangno, 1998: Microstructures of low and middle-level clouds over the Beaufort Sea. *Quart. J. Roy. Meteor. Soc*., **124**(550), 2035–2071, doi: 10.1002/qj.49712455012.

Hudson, J. G., and S. S. Yum, 2001: Maritime-continental drizzle contrasts in small cumuli. *J. Atmos. Sci*., **58**(8), 915–926, doi: 10.1175/1520-0469(2001)058<0915:MCDCIS>2.0.CO;2.

Hudson, J. G., and S. S. Yum, 2002: Cloud condensation nuclei spectra and polluted and clean clouds over the Indian Ocean. *J. Geophys. Res*., **107**(D19), INX2 21-1–INX2 21-12, doi: 10.1029/2001JD000829.

IPCC, 2007: Summary for Policymakers. *Climate Change 2007*: *The Physical Science Basis*, *Contribution of Working Group I to the Fourth Assessment Report of the Intergovernmental Panel on Climate Change*, Solomon et al., Eds., Cambridge University Press, Cambridge, United Kingdom and New York, NY, USA.

Jaffe, D., I. McKendry, T. Anderson, and H. Price, 2003: Six "new" episodes of trans-Pacific transport of air pollutants. *Atmos. Environ*., **37**(3), 391–404, doi: 10.1016/S1352-2310(02)00862-2.

Konwar, M., A. S. Panicker, D. Axisa, and T. V. Prabha, 2015: Near-cloud aerosols in monsoon environment and its impact on radiative forcing. *J. Geophys. Res.*, **120**, 1445–1457, doi: 10.1002/2014JD022420.

Konwar, M., R. S. Maheskumar, J. R. Kulkarni, E. Freud, B. N. Goswami, and D. Rosenfeld, 2012: Aerosol control on depth of warm rain in convective clouds, *J. Geophys. Res.*, **117**(D13), D13204, doi: 10.1029/2012JD017585.

Liu, P. F., C. S. Zhao, P. F. Liu, Z. Z. Deng, M. Y. Huang, X. C. Ma, and X. X. Tie, 2009: Aircraft study of aerosol vertical distributions over Beijing and their optical properties. *Tellus B*: *Chemical and Physical Meteorology*, **61**(5), 756–767, doi: http://dx.doi.org/10.1111/j.1600-0889.2009.00440.x.

Miles, N. L., J. Verlinde, and E. E. Clothiaux, 2000: Cloud droplet size distributions in low-level stratiform clouds. *J. Atmos. Sci*., **57**, 295–311, doi: 10.1175/1520-0469(2000)057<0295:CDSDIL>2.0.CO;2.

Noone, K. J., and Coauthors, 1992: Changes in aerosol size- and phase distributions due to physical and chemical processes in fog. *Tellus B*: *Chemical and Physical Meteorology*, **44**, 489–504, doi: http://dx.doi.org/10.3402/tellusb.v44i5.15563.

Prabha, T. V., A. Khain, R. S. Maheshkumar, G. Pandithurai, J. R. Kulkarni, M. Konwar, and B. N, Goswami, 2011: Microphysics of premonsoon and monsoon clouds as seen from in situ measurements during the Cloud Aerosol Interaction and Precipitation Enhancement Experiment (CAIPEEX). *J. Atmos. Sci*., **68**, 1882–1901, doi: 10.1175/2011JAS3707.1.

Rangno, A. L., and P. V. Hobbs, 2005: Microstructures and precipitation development in cumulus and small cumulonimbus clouds over the warm pool of the tropical Pacific Ocean. *Quart. J. Roy. Meteor. Soc*., **131**, 639–673, doi: 10.1256/qj.04.13.

Seinfeld, J. H., and S. N. Pandis, 1997: *Atmospheric Chemistry and Physics: From Air Pollution to Climate Change*, Wiley-Interscience, 444–445.

Stith, J. L., J. Haggerty, C. Grainger, and A. Detwiler, 2006: A comparison of the microphysical and kinematic characteristics of mid-latitude and tropical convective updrafts and downdrafts. *Atmos. Res*., **82**, 350–366, doi: 10.1016/j.atmosres.2005.12.008.

Twomey, S., and T. A. Wojciechowski, 1969: Observations of the geographical variation of cloud nuclei. *J. Atmos. Sci.*, **26**, 648–651, doi: 10.1175/1520-0469(1969)26<648:OOTGVO>2.0.CO;2.

Zhang, Q., C. S. Zhao, X. X. Tie, Q. Wei, M. Y. Huang, G. H. Li, Z. M. Ying, and C. C. Li, 2006: Characterizations of aerosols over the Beijing region: A case study of aircraft measurements. *Atmos. Environ*., **40**, 4513–4527, doi: 10.1016/j.atmosenv.2006.04.032.

Zhang, Q., J. N. Quan, X. X. Tie, M. Y. Huang, and X. C. Ma, 2011: Impact of aerosol particles on cloud formation: Aircraft measurements in China. *Atmos. Environ*., **45**, 665–672, doi: 10.1016/j.atmosenv.2010.10.025.